Electron Microscopy --Now in Color

Pirozzi, Nicole

DOI:
10.33612/diss.222300319


4ª

Probes for ColorEM in cells and tissues

Nicole M. Pirozzi, Jeroen Kuipers, Ben N.G. Giepmans

ABSTRACT

Analytical electron microscopy (EM) can image chemical content of biological samples at high resolution. To increase the probe toolbox for multi-color EM with energy dispersive X-ray (EDX) analysis, elemental probes are explored. This chapter evaluates exogenous elements added through metallo-pharmaceuticals, immunolabeling, metal incorporation in enzymatic reactions, tissue staining, organelle-specific fluorescent probes. At this time, metallopharmaceuticals and immunolabeling with nanoparticles are most readily applicable as EDX probes. With further development, other methods described could be used to bring additional color and information to EM.

INTRODUCTION

Imaging the basic building blocks of life is imperative to understand biology in health and disease. Identification of subcellular features at the ultrastructural level is key to unravel how molecules and organelles regulate cellular processes. Analytical signals that pinpoint the presence of certain atoms at high resolution may aid identification of cellular features in electron microscopy (EM). The combination of characteristic atomic signatures as color overlays with EM data is popularly termed ColorEM[1] and is achieved with methods like elemental detection via energy dispersive X-ray (EDX) imaging.[2] Application of EDX in life sciences is gaining popularity but there has been limited exploration of probes with EDX-specific signals. Use of such probes in multiplex imaging has high potential: Multiple probes with unique, exogenous elements can be utilized in a single sample to visualize many targets in a single image. ColorEM's detection of endogenous signals and elemental probes are analogous to fluorescent light microscopy's nuclear staining and immunofluorescence but with greater spectral range. In this chapter we determine the feasibility of elemental labeling by several targeting methods in biosamples.

RESULTS & DISCUSSION

EDX imaging of intracellular platinum from cisplatin exposure

Metallopharmaceutical localization within cells through ColorEM is explored with cisplatin. Cisplatin, with one platinum atom per molecule (**Figure 1A**), is commonly used to treat many cancers.[3] Because the current understanding of cisplatin's cellular damage is mainly derived from protein interaction studies in cell-free environments[4], high resolution imaging of platinum atoms could shed light on the cellular processing of the metallopharmaceutical. Here, we explore if we can localize the exact whereabouts of cisplatin using EDX in exposed HeLa cells.

Platinum of cisplatin can be detected by the characteristic X-rays platinum emits upon electron beam irradiation (**Figure 1B**). HeLa cells were exposed to cisplatin in culture followed by fixation and EM sample preparation. Platinum detection via EDX imaging is not immediately clear (**Figure1C**) and requires higher magnification imaging (**Figure 1D**). Further investigation of electron-dense perinuclear structures, marked by arrows in **Figure 1C**, reveals concentrated platinum signal. One perinuclear structure is shown in **Figure 1D** exhibiting several subcellular structures relatively rich in platinum. The largest platinum-rich structure is likely a lysosome, based on ultrastructure.

Spectral analysis (**Figure 1E**) of platinum-rich regions compared to neighboring regions confirm the platinum signal from Mα (2.050 keV) and Lα (9.442 keV) characteristic X-ray lines. Detection of platinum Mα at 2.05 keV is difficult due to its spectral proximity to phosphorus (Kα at 2.01 keV) and osmium (Mα at 1.91 keV) which are in higher abundance in embedded cells. In **Figure 1E**, the normalized counts of the map sum of the platinum-rich region are much higher around 2.0 keV than the total map sum and the sum of the neighboring region. In the higher energy range (**Figure 1E**), the spectra of the platinum-rich region and map sum show much more signal than that of the neighboring region around 9.5 keV. The peak of the spectrum of the platinum-rich region confirms that the region has relatively more signal from platinum Lα than the map sum, albeit, likely with a small spectral shift. The signal localization of phosphorus and osmium maps are not identical to each other, nor to the platinum map (**Figure 1D**), which supports correct signal spectral differentiation. The central lysosome is rich in osmium because of its many membranes. The co-localization of chlorine reflects a chlorine artifact in EPON-embedded tissue[5], and not a co-localization of cisplatin (**Figure 1D**), even though the molecule contains two chlorine atoms (**Figure 1A**). Strikingly, the platinum map has high localization with the sulfur map (**Figure 1D**), which might be due to platinum's high reactivity with sulfhydryl groups.[6]

Cisplatin imaging has recently been performed by correlating confocal microscopy with secondary ion mass spectroscopy on the nanoscale (NanoSIMS[7]) to bring cisplatin imaging to the single cell level.[8,9] Other attempts at ultrastructural cisplatin localization include using cisplatin as a negative stain, blocking subsequent uranyl acetate staining of heterochromatin.[10] Platinum detection through EDX imaging of cisplatin-exposed cells is successful. Cell exposure to 250 μM of cisplatin was optimized for EDX detection, with no platinum observed in cells exposed to lower concentrations (≤125 μM) and cell death observed at higher concentrations (500 μM). Even with this relatively high concentration of cisplatin, platinum detection is on the edge of detection at lower magnification (**Figure 1C**). Higher acceleration voltage and magnification is achieved with a transmission electron microscope (TEM) than with a scanning electron microscope (SEM). While EDX imaging in a SEM is sometimes sufficient, for conclusive platinum detection, the TEM system is required. Unsuccessful EDX platinum detection reported in cells[11] could have been because Lα detection was not feasible due to the use of a SEM system with restricted acceleration voltage. Use of maximized cisplatin concentrations and a capable EDX system contribute to the success of platinum detection in cisplatin-exposed cells.

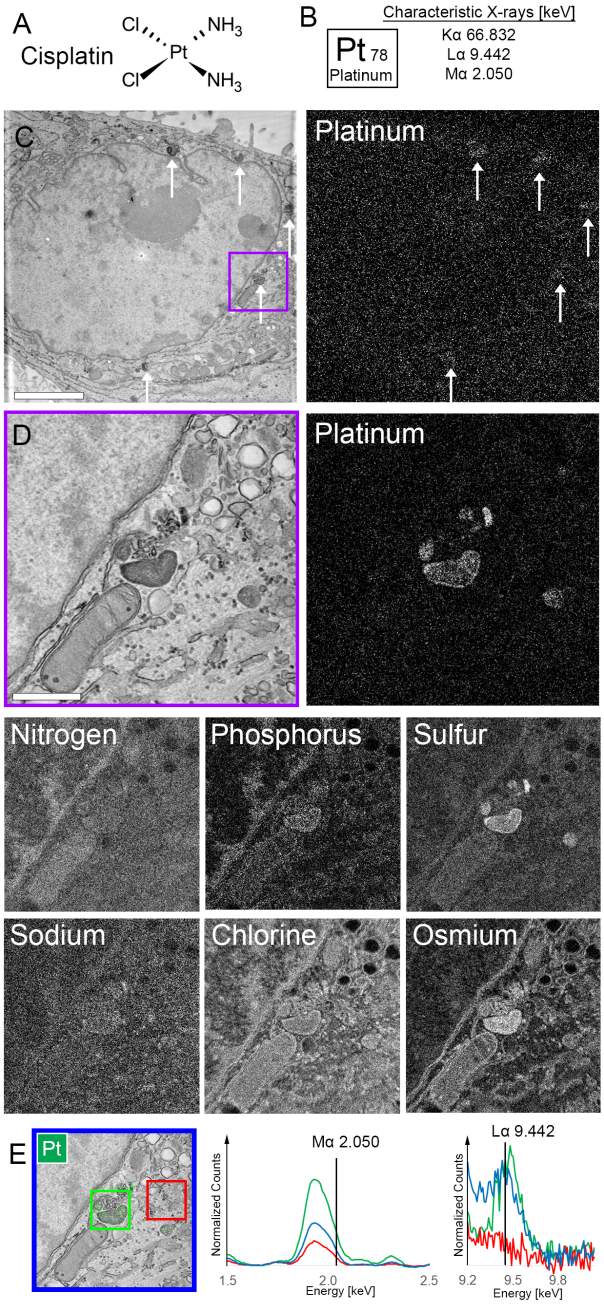

◀Figure 1. Metallopharmaceutical cisplatin is localized to dense bodies. Platinum detection of cisplatin-exposed cells in thin-section, resin-embedded samples demonstrates the proof of concept of probes from cell culture to EDX signal. **(A)** Cisplatin contains one platinum atom **(B)** which has the noted characteristic X-ray energies. **(C)** HeLa cells exposed to cisplatin have electron-dense structures around the nucleus with slight platinum signal (arrows). **(D)** Enlarged region boxed in (C) shows one of the perinuclear structures. EDX imaging shows platinum signal in structures of interest as well as sulfur, osmium, chlorine, and some phosphorus. **(E)** Spectral comparison of areas with high (green) and low platinum signal (red), as well as the total map sum (blue) confirm the platinum signal. Platinum's spectral proximity (Mα) to phosphorus and osmium make detection difficult at lower energies. The platinum signal is clearer from the Lα energy line at 9.442 keV. Bars 2.5 µm (C), 0.5 um (D).

Immunolabeling: limits on particle size and metal-enhancement

Specific biomolecules can be identified within EM cellular ultrastructure through antigen targeting with an electron-dense label. Gold particles are the most common immuno-targeted label for EM[12] with recent developments in Quantum Dots for their stable fluorescence allowing multimodal imaging[13], and increased labeling efficiency.[14] Nanoparticles ≥10 nm in diameter are popular because particles < 10 nm in diameter become difficult to discern from contrasted subcellular features, and much larger particles decrease labeling efficiency and cause more ambiguity in estimating target localization. Elemental imaging with EDX could alleviate the difficulties with identification of smaller particles but the particle size limit has yet to be investigated.

Identification of multiple targets relies on the ability to differentiate labels. Traditionally, multiple targets are identified by varied sizes of gold nanoparticles, but this is limited to three targets at most. Differentiation of particles in double labeling experiments with gold particles and Quantum Dots can be done through manual analysis of shape and electron density, image processing[15], or EDX imaging.[2] Multiplexing immuno-targeted labels could employ antibodies conjugated to nanoparticles of different materials or use various metal enhancements to add discriminative signal. Silver enhancement has been used to enlarge small gold nanoparticles for increased visibility in EM.[16] Here, we investigate the gold particle sizes suitable for detection and proof-of-concept use of silver enhancement for EDX imaging.

Gold nanoparticles of three different sizes are detectable via EDX imaging. Gold particles of 10 nm diameter are the most prominently visible in the EM image (**Figure 2A**), as expected, with clear gold signal in the EDX map. Particles of 5 nm diameter are also clear in EM and EDX (**Figure 2B**). Gold particles of 2 nm diameter are not clearly visible in the EM (**Figure 2C**) and require higher magnification in EM and EDX for signal to emerge in the gold EDX map. While the detection of 2 nm gold is successful, the high magnification required is unfavorable for typical biological EM studies. Silver enhancement of 2 nm gold particles is positive in silver signal in the EDX map without detection of the 2 nm gold beneath (**Figure 2D**). The gold plus silver particles are approximately 30 nm in diameter. With a 2 nm pixel size for EDX imaging, the amount of silver and X-ray signal thereof likely overpowers any gold signal. Tuning the strength/amount of the silver enhancement would be interesting for future investigations.

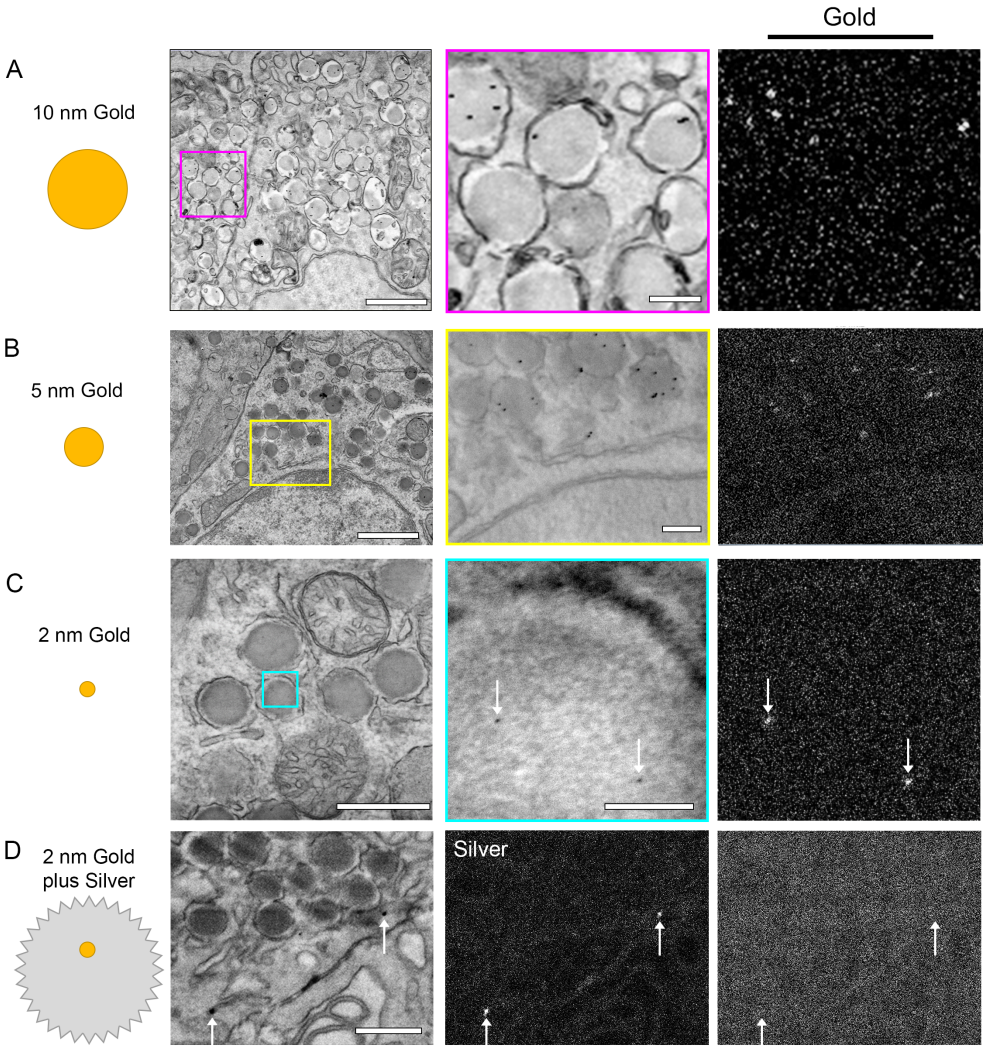

Figure 2. Small immuno-targeted nanoparticles and EDX imaging localize targets at the ultrastructural level. Immunolabeling with nanoparticles with diameters ≥ 10 nm are easily detected by their elemental content, as seen by anti-insulin labeling with 10 nm gold **(A)**. **(B-C)** Smaller gold particles of 5 nm and 2 nm (arrows) in diameter, shown labeling glucagon, are detectable at higher magnification. **(D)** Gold nanoparticles labeling glucagon are enlarged by silver enhancement (arrows), resulting in EDX detection of silver but no detectable gold. Bars: 1 µm (A, B); 0.5 µm (D); 0.2 µm (A-enlarged, B-enlarged, C); 0.05 µm (C-enlarged).

Silver enhancement introduces discriminative signal that can be used for immuno-targeting differentiation. Investigation of silver-enhanced gold followed by an additional gold immunolabelling was intended but not completed. It is unclear whether the chemically stability of the silver enhancement can withstand an additional gold immunolabelling. Alternatively, a subsequent labeling could be performed on the opposite side of a tissue section, in which case the necessary sample holder would be a grid without a supportive film. Gridded sample holders, will likely increase elemental signal from the grid material. Sample holder artifacts are more pronounced in the SEM system and therefore, use of a TEM system is recommended. Gold nanoparticles as small as 2 nm can be detected at high magnification and silver enhancement of gold has the potential to add discriminative signal for EDX imaging.

Metal-incorporation in diaminobenzidine reaction precipitates

Peroxidases, such as horseradish peroxidase (HRP), catalyze hydrogen peroxide-oxidation of 3,3′-Diaminobenzidine (DAB), to form a brown/electron-dense precipitate at the site of the peroxidase, visible with light microscopy (LM) and EM.[17] Peroxidases conjugated to fluorescent proteins have been developed as genetically-encoded CLEM probes; fluorescent indicator and peroxidase for precipitation with EM resolution (FLIPPER).[18] Metal-incorporated DAB precipitates have been used in ColorEM by energy filtered transmission EM.[19] Peroxidase reactions can be enhanced by adding cobalt and/or nickel ions,[20] which suggest that these metallic ions are easily incorporated into the reaction. Detection of these and other ions, after introduction to DAB reactions are explored with EDX.

Cells expressing an ER-FLIPPER probe undergo a DAB reaction in the presence of metals to add discriminative signal in EDX imaging. Of the 8 metallic salts added during precipitate reactions, three are retained (**Table 1**). Genetically-encoded DAB-tags are osmium-philic and therefore clear in EM, as shown here localized to the endoplasmic reticulum (ER; **Figure 3A**). Imaging of the nickel- and cobalt-incorporated DAB precipitate exhibits a proof-of-concept example that elemental probes in the DAB reaction are retained through dehydration, resin embedding, and EM sample preparation. The precipitate is nitrogen-rich and readily binds with osmium, thus the ER stands out in EDX nitrogen and osmium maps (**Figure 3A**). Spectroscopy measurements, shown by the map sum (**Figure 3B**), display the cobalt and nickel signals which are marginally above background in lower energies (Lα) but more prominent in higher energies (Kα). The aim of adding metals to DAB precipitates is to use the elemental signature to discriminate multiplexed labels. Unfortunately, the metals appear to compete for binding sites within DAB precipitates: The subsequent application of one ion, replaces the previous ion. EDX imaging of multiplexed

metal-incorporation in DAB precipitates is not possible via this method but, it may still be possible with elemental conjugation to DAB[19,21] or with DAB-shielding treatments[22] to seal the elemental incorporation. Metal-incorporation in precipitate reactions is retained and detected but further development is necessary to enable multiplexing for EDX imaging.

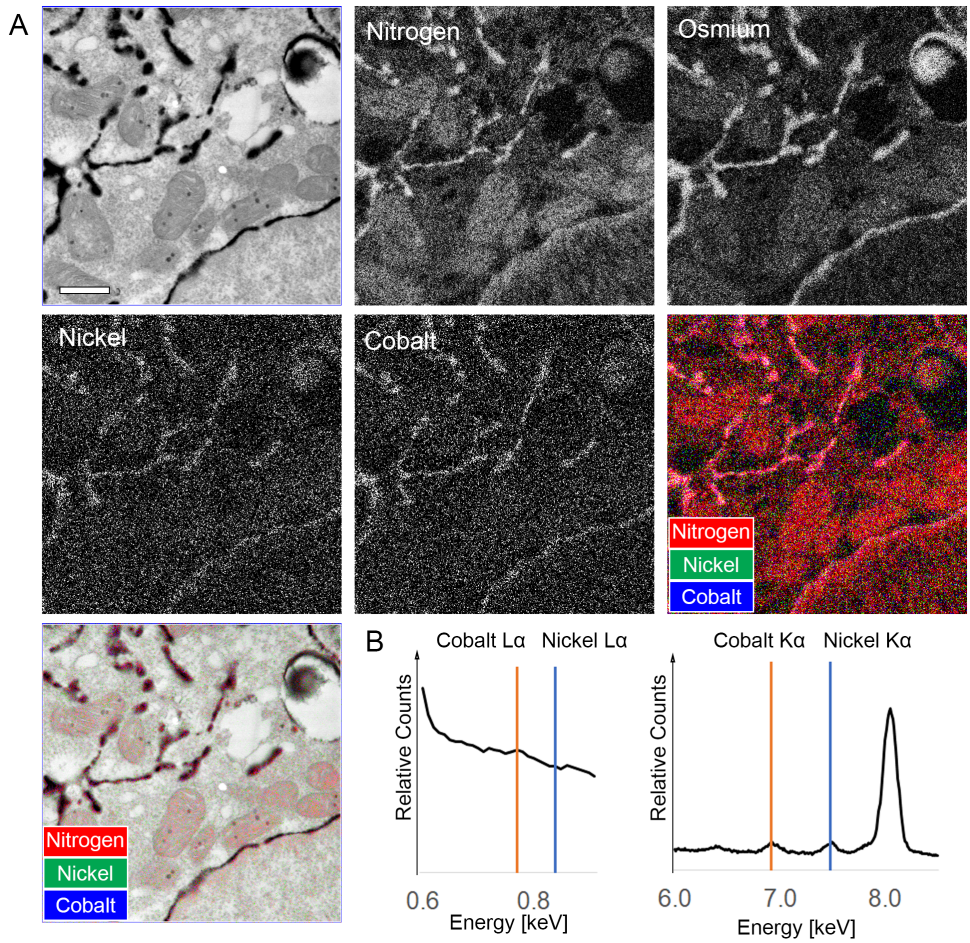

Figure 3. Metals incorporated at precipitate formation are detected through EDX imaging. (A) Endoplasmic reticulum genetically labeled with a peroxidase undergoes a 3,3′-diaminobenzidine (DAB) reaction in the presence of cobalt and nickel, the metals are incorporated into the osmiophilic precipitate. The DAB precipitate is visible by the bold, electron-dense structures in the cytoplasm and along the nuclear envelope (nucleus located at bottom left). DAB precipitates are typically rich in nitrogen and osmium. Through exposure to nickel and cobalt during formation, the precipitates retain the metals through sample preparation to be visualized with EDX. **(B)** The presence of nickel and cobalt are seen by their peaks in the map sum spectrum where clear signal is seen in the higher energy Kα lines, verifying elemental presence in the sample region. Bars: 0.5 µm.

Table 1: Incorporation of metals in DAB precipitates

Compound	Element (symbol)	DAB affinity
$CoCl_2$	Cobalt (Co)	Yes
$NiSO_4$	Nickel (Ni)	Yes
$CuSO_4$	Copper (Cu)	Yes
$MnCl_2$	Manganese (Mn)	No
$HfCl_4$	Hafnium (Hf)	No
$Pb(NO_3)_2$	Lead (Pb)	No
$CeCl_3$	Cerium (Ce)	No
$Sm(CH_3CO_2)_3$	Samarium (Sm)	No

Stains to paint cellular features in EDX

Exogenous elements via contrast-inducing EM stains add discriminative signal to biological tissue. The most popular contrasting agents contain osmium, uranium, and lead. Here, we demonstrate the ability to map the individual stains to 'paint' an EM image. **Figure 4** shows a contrasted sample with EDX imaging revealing each stain's contribution to the electron-density seen in the EM image. Rat pancreas is shown (**Figure 4**) with standard EM sample preparation including post-fixation with osmium tetroxide and post-embedding contrasting with uranyl acetate and Reynold's lead citrate. The region imaged is the border of an islet of Langerhans with the exocrine cells above and endocrine cells below. The nitrogen map reflects the endogenous signal from high concentrations of proteins and densely packed DNA. Osmium tetroxide has reactivity to lipids, showing clear membranes (**Figure 4**, Osmium). Uranium is generally unspecific, but has slight affinity to heterochromatin and collagen (**Figure 4**, Uranium), and is also present in the secretory granules of exocrine cells and the left-most endocrine cell, an alpha cell. The islet is encapsulated by a collagen-rich barrier-seen in the uranium map (**Figure 4**). Lead tends to bind to all osmium and uranium present in the sample (**Figure 4**, Lead). The overlay of the three metals gives an impression of how metallic stains could be used to paint cellular features.

The capability of EDX to differentiate the stains, along with recent development of alternative contrasting agents (e.g. neodymium[23,24]) inspires this explorative approach toward staining to identify subcellular features in EDX. Some compounds have been reported to add contrast, such as phosphotungstic acid's use as a post-embedding contrasting agent prior to uranyl acetate staining[25] and hafnium chloride for EM contrast in plant cells.[26] Other elements that add no additional electron density to the image still have EDX painting potential, such as mercury chloride which was recently imaged in fish using

X-ray fluorescence.[27] We determine if EDX imaging can be used to measure the relative concentration of exogenous elements, irrespective of added electron density, aimed to discover elemental paints that can be used to identify cellular features and/or organelles. Metallic compounds are explored to add exogenous elemental signal to distinct cellular features. Compounds and their ability to add discriminative signal in rat pancreas tissue via detection of 10 different elements are summarized in **Table 2**. Distinct localization of added elements is seen in tissue stained with lead citrate, phosphotungstic acid, hafnium chloride, and iridium bromide (**Figure 5A-E**). Lead citrate (**Figure 5A**) binds only to the osmium-fixed membranes, showing less signal than when applied after uranium contrasting (**Figure 4**). Phosphotungstic acid has a strong presence in the nuclei and secretory granules of some exocrine cells (**Figure 5B**). Hafnium chloride signal is seen in heterochromatin, and the membranes of the ER (**Figure 5C**). Confirmation of the elemental signals is seen in the map sum spectra (**Figure 5A-C**).

Iridium bromide shows positive signal for both iridium and bromine (**Figure 5D-E**). Bromine appears to bind at the exocrine granules, and slightly to heterochromatin. Iridium seems to bind to all membranes, as well as heterochromatin and exocrine granules, omitting only euchromatin. Detection of bromine Lα (1.48 keV) conflicts with aluminum Kα (1.49 keV), which should be considered when choosing a microscope sample holder. Iridium detection in the SEM is restricted to Mα (1.98 keV) which has close spectral proximity to phosphorus Kα (2.01 keV), thus further analysis should be performed on the TEM system to collect iridium Lα (9.18 keV) characteristic X-rays.

A few metallic compounds (samarium acetate, lanthanum nitrate, and gadolinium acetate) are detected in the map sum spectrum but show no specific localization in the map (**Figure 5F-H**), indicating that the tissues are homogeneously stained. Drift correction during EDX imaging in the SEM with AZtec software depends on the type 2 secondary electron detector (SE2) image. Imaging the sample stained with gadolinium acetate was repeatedly discontinued by the software due to very low SE2 image contrast. Of all imaging attempts, the highest gadolinium signal is observed in a scan consisting of only 7 frames, therefore, gadolinium acetate tissue staining should be further analyzed and/or imaged in a TEM system in future studies for more conclusive results. Sodium orthovanadate and mercury chloride are detected in neither the elemental map nor the map sum spectrum (**Figure 5I-J**), indicating that little or none of the compounds are retained after tissue staining. There is opportunity for metallic stains for EDX imaging and future studies should also consider tissue staining variables such as concentration, pH, temperature.

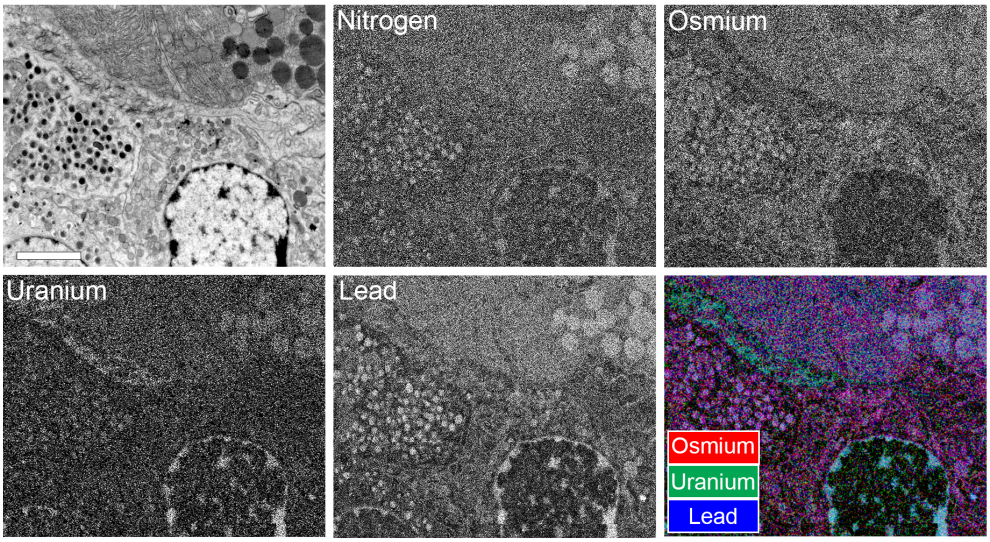

Figure 4. Routine contrast agents 'paint' cellular features with elemental imaging. Rat pancreas post-fixed with osmium tetroxide and contrasted with uranyl acetate and lead citrate is imaged with EM and EDX to differentiate the added elements. The EDX nitrogen map shows endogenous composition of protein-rich secretory granules of the exocrine (upper right) and endocrine (lower) pancreas. Osmium is seen in all membranes/lipids, uranium stains the sample non-specifically with slight affinity to heterochromatin in the nucleus (lower right) and the collagen (upper left), and lead is a non-specific amplifier of the osmium and uranium signal. The color overlay conveys the prevalence of each compound bound to specific cellular features. Bars 2.5 µm.

Table 2: Metal stains for EDX

Compound	Element of interest (Symbol)	Map detection	Spectrum detection	Imaging frames
Lead citrate	Lead (Pb)	++	++	32
Phosphotungstic acid	Tungsten (W)	++	++	15
Hafnium chloride	Hafnium (Hf)	+	++	31
Iridium bromide	Bromine (Br)	+	++	15
Iridium bromide	Iridium (Ir)	+	+	15
Samarium acetate	Samarium (Sm)	-	++	41
Lanthanum nitrate	Lanthanum (Ln)	-	++	20
Gadolinium acetate	Gadolinium (Gd)	-	+	7
Sodium orthovanadate	Vanadium (V)	-	-	17
Mercury chloride	Mercury (Hg)	-	-	15

Detection is level is noted as negligible (-), present (+), and strong (++).

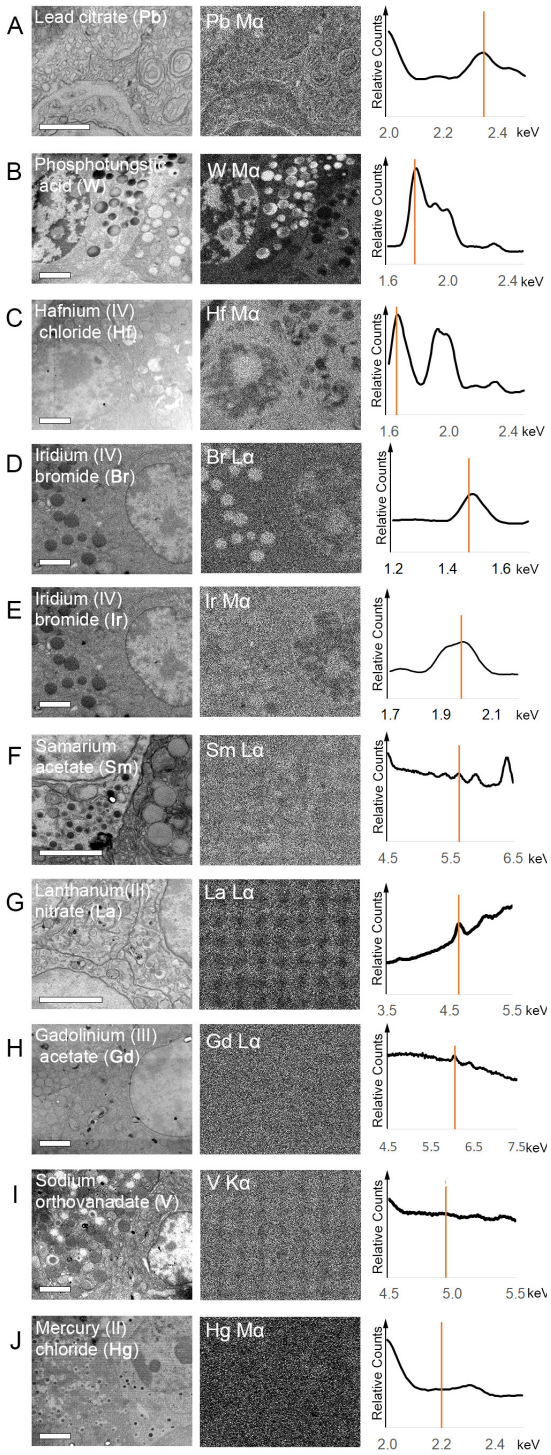

◀Figure5. Tungsten, hafnium, and bromine 'paint' cellular features. Rat pancreas was stained with noted compound before EPON-embedding. EM image, EDX map of added element, and map sum spectra (black) with line (orange) indicating the spectral location of the elemental map are shown. Contrast due to the added element is seen in the EM image. **(A-E)** Elemental compounds had positive signals in the elemental maps. **(F-H)** Added compounds showed no localized signal in the elemental maps, but their presence in the sample is shown by the map sum spectra. **(I-J)** These elements do not appear to be present in the imaged tissue. Phosphotungstic acid, hafnium chloride, and iridium bromide have the potential to add discriminative signal to EDX imaging. Bars: 2 μm.

Fluorescent Probes

Organelle or molecular identification is standard in LM with fluorescent probes. The ultrastructural context, however, is dependent on LM-EM data correlation which is subject to a resolution gap and registration issues. There is a need for organelle-labeling probes that are detectable at EM resolution, aiding ultrastructural organelle identification. Commonly used fluorescent probes for mitochondria, lysosome, and ER tracking are explored here for EDX detection. MitoTracker and LysoTracker probes contain chlorine and fluorine atoms but the sensitivity of EDX to detect the probes over low background endogenous levels remains unknown. Fluorescent organelle-targeted probes synthesized with metal ion complexes[28], such as ReZolve-ER [29] and IraZolve- Mito[30], offer increased photostability and add exogeneous elements for potential detection with EDX. Rhenium in mitochondria-targeted fluorescent probes was recently reported to have been detected by X-ray fluorescence.[31] In addition, we use fluorine-containing BODIPY Cholesterol and attempt probe addition via post-embedding immuno-labeling with fluorine-containing ATTO 514. These techniques are appraised for their potential use with EDX imaging.

No probe is detected in EDX imaging (**Table 3**, **Figure 6**). The MitoTracker-labeled cells were embedded in Durcupan resin to avoid an EPON-dependent chlorine artifact.[5] Still, no chlorine is detected in the mitochondria and slight signal in the lysosomes and nuclear envelope is observed (**Figure 6A**). Detection of the fluorine atoms of LysoTracker is also unsuccessful, with unexpected detection of fluorine in the nucleolus of the analyzed cell (**Figure 6B**). Another LysoTracker probe, LysoTracker Red DND-99, with manufacturer claims of probe retention after chemical fixation is used but, again, no fluorine is detected. While probes may be held by fixation, it is not clear if the probes remain after EM processing, namely dehydration and embedding. Rhenium and iridium from ReZolve ER and IraZolve Mito are not detected (**Figure 6C-D**), and the ultrastructure appears compromised from the probes. Interestingly, IraZolve-treated cells show iridium signal in the lysosomes, similar to chlorine in the MitoTracker sample, potentially suggesting degraded, non-fluorescent accumulation of the probe within degradative compartments.

To achieve the goal of specific organelle-labeling, alternative sample processing was performed using high pressure freezing (HPF) and freeze substitution (FS) techniques for cells exposed to LysoTracker, ReZolve ER, and IraZolve Mito. Cells embedded in HM20 show no improvement in detection of the elements of interest (data not shown). BODIPY Cholesterol detection via fluorine does not succeed (**Figure 6E**), even with alternate fixation using aldehydes with 0.1% digitonin, primary osmium fixation, and a combination of osmium-aldehyde fixation. Cells fixed in osmium-aldehyde appear to have increased lipid retention yet no fluorine is detected (**Figure 6E**). None of the fixation methods changes the outcome, leaving retention/detection of BODIPY Cholesterol inconclusive.

To determine if the detection failures are due to lack of retention or sensitivity, a post-embedding immunolabeling approach is employed with Atto 514, which has 6 fluorine atoms per molecule. Amylase in rat pancreas exocrine tissue is targeted (**Figure 6F**), but EDX imaging yields no conclusive results, even at a higher magnification (data not shown). Other immuno-targets and biotin-streptavidin amplification of Atto 514 were attempted (data not shown), but no better outcome was achieved. The question remains whether the lack of detection is due to sensitivity or probe retention. Probe retention could be addressed by fluorescence imaging after HPF/FS[32], but immunolabeling approaches suggest that sensitivity is the issue, especially with light atoms like fluorine which are more difficult to detect than heavier atoms. The probes with metal ion complexes show the most promise but probe retention must first be achieved.

Table 3: Fluorescent probes listed with the concentration used in culture with HeLa cells and the elements of interest.

Probe	Concentration in culture (µM)	Number of atoms of interest/molecule
MitoTracker Green FM (Invitrogen)	0.10	5 chlorine
LysoTracker Green DND-26 (Invitrogen)	0.05	2 fluorine
LysoTracker Red DND-99 (Invitrogen)	0.10	2 fluorine
ReZolve-ER (ReZolve Scientific)	100	1 rhenium
IraZolve-Mito (ReZolve Scientific)	50	1 iridium
BODIPY Cholesterol (Avanti Lipids)	0.10	2 fluorine
Atto 514 (ATTO-TEC)	N/A Immunolabeling	6 fluorine

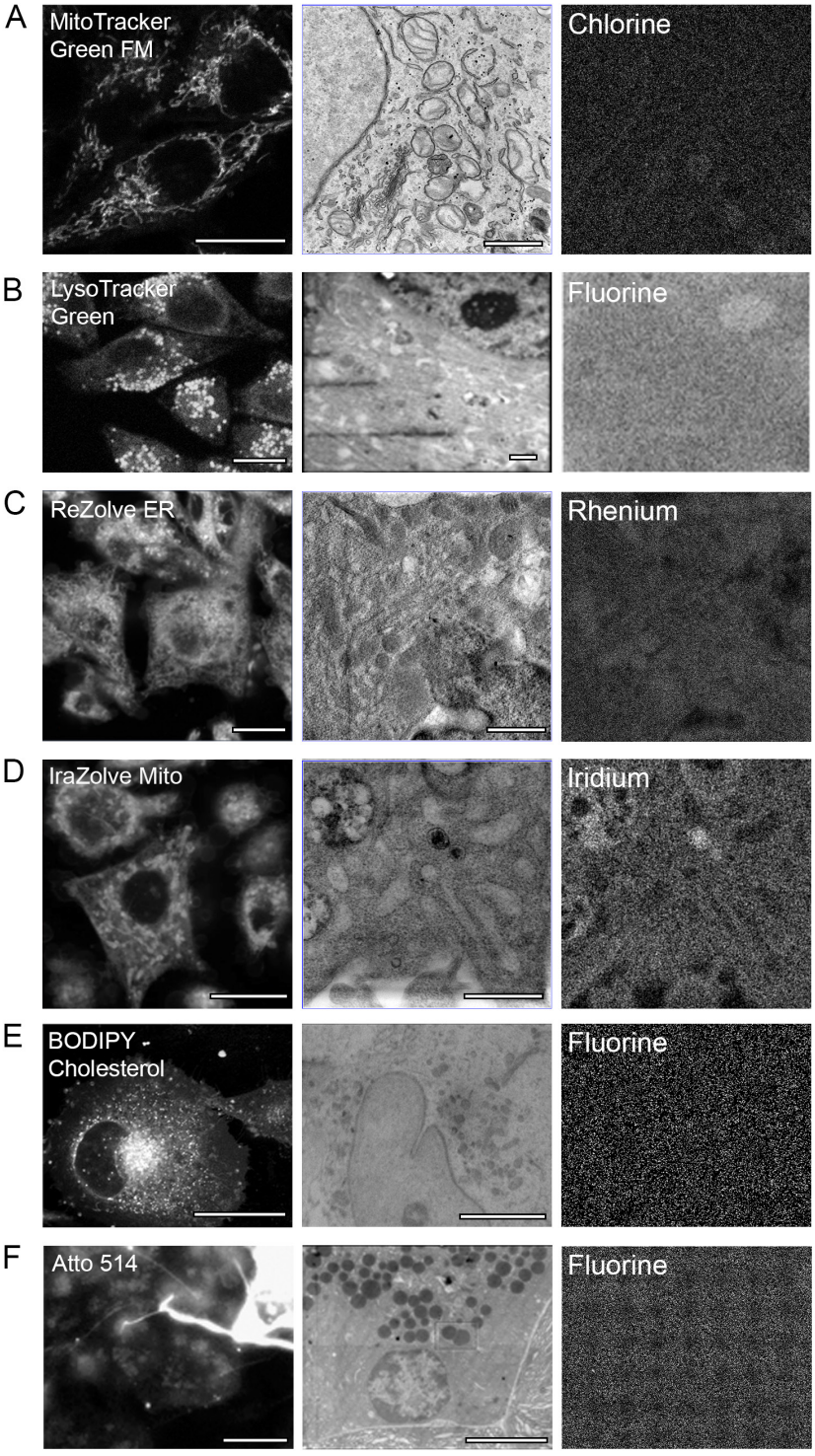
A
MitoTracker Green FM
Chlorine
B
LysoTracker Green
Fluorine
C
ReZolve ER
Rhenium
D
IraZolve Mito
Iridium
E
BODIPY - Cholesterol
Fluorine
F
Atto 514
Fluorine

◄**Figure 6. Fluorescent molecular probe detection is not (yet) possible with EDX**. Several commercially-available fluorescent probes were imaged by their elemental signatures with EDX. The first column of images are the fluorescence images of the probes, followed by the EM image, and the EDX elemental map of the map of interest shown in the EM image. **(A)** MitoTracker, which binds to mitochondria in cells, was not detected by its chlorine atoms. The chlorine map shows no distinct signal in mitochondria (aligned in center) but a slight increase in lysosomes and at the nuclear membrane (left). **(B)** EDX imaging of LysoTracker, which localizes to acidic lysosomes (several electron-dense structures in the cytoplasm in EM), revealed no fluorine signal in lysosomes but striking fluorine signal in the nucleolus of the nucleus (above). **(C)** ReZolve-ER binds to the endoplasmic reticulum (ER) of cells. The rhenium elemental map shows no distinct signal in any feature resembling ER but slight increase of rhenium signal in the heterochromatin of the nucleus (lower right) and mitochondria. **(D)** IraZolve Mito localizes to the mitochondira of cells, as seen by the fluorescence image. A region was imaged with EDX where many mitochondria were present but iridium signal was only seen in lysosomes. **(E)** BODIPY cholesterol is a fluorophore-labeled cholesterol molecule that appeared in many membranous structures but EDX analysis of these cells produced no clear fluorine signal. **(F)** Atto 514 was used as a secondary antibody for anti-amylase labeling. EDX imaging shows no fluorine signal in the labeled secretory granules of the exocrine cell. Bars: 20 µm (fluorescent images); 1 µm (A, B, C, D); 5 µm (E, F).

CONCLUSION

EDX imaging in biology applications shows promise. Imaging of cisplatin metabolized within cells is a novel observation enabled by ColorEM. This experiment was proof-of-concept that a compound added to cells in culture could be detected by its elemental signature in a resin-embedded thin section. EDX can potentially be used for investigations of cisplatin or other metallopharmaceuticals. Elemental maps are the most valuable read-out in EDX imaging experiments, displaying the location of relative concentration where the elements of interest have little or no peaks in the map sum, such as with small immunolabels. Imaging nanoparticles with EDX is successful. Although the method is restricted to the particle size/magnification necessary for detection and dependent on immuno-targets and nanoparticles available, the results are hopeful. Map sum spectra were useful for stains, to indicate if the stain was retained in the tissue. Other methods described, namely metal-incorporation in DAB precipitates, elemental paints, and use of fluorescent probes, need further development before (routine) use. Continued development of ColorEM probes and tools is necessary to achieve cellular feature identification at EM resolution.

METHODS

Cisplatin in HeLa cells

HeLa cells were exposed to 250μM cisplatin in culture for 19 hours then fixed and prepared for EM. Cells were fixed with 2% glutaraldehyde/ 2% paraformaldehyde dropwise and then refreshed with complete fixative. Cells were post-fixed with 1% osmium tetroxide for 30 min, embedded in EPON, and cut into 100-nm thick sections with a Leica EM UC7 Ultramicrotome (Leica Microsystems, Vienna, Austria) and a diamond knife (Diatome Ltd, Nidau, Switzerland).

A section of 100 nm thickness without further contrasting was imaged in the TEM system at 200 keV. EDX was performed on a Talos F200x transition EM (Thermo Fisher, Eindhoven, Netherlands) operated in STEM- mode with EDX imaging acquired by four SuperXG1 silicon drift detectors, hereinafter referred to as the TEM system.

EDX scans where acquired at 45.5k magnification, 512 by 512 pixels, 10 μs dwell time, 5.29 nA current, and ~250 frames. Brightness and contrast of EM images and elemental maps were linearly adjusted in Adobe Photoshop for all figures. Spectra were normalized at 1.6-1.7 keV in the lower energy spectra and 9.8-9.9 keV in the higher energy spectra.

Immunolabeling with gold

Rat pancreas tissue was cut into 1 mm^3 cubes and submerged in 2% glutaraldehyde/ 2% paraformaldehyde. Fixed tissue was cut into 50 μm tissue sections and post-fixed with 1% osmium tetroxide for 1 hour. Tissue was embedded in EPON and cut into 100-nm thick sections onto Formvar coated 1 mm hole nickel grids.

Post-embedding immunolabeling was performed on droplets on Parafilm. First, the girds were etched with 1% periodic acid for 10 min, followed by 4 times rinsing with MilliQ. Blocking was done with 1% bovine serum albumin (BSA) for 30 min. The grids were incubated with 1:50 mouse anti-glucagon in 1% BSA for 2 hours, rinsed with tris-buffered saline 4 times, and then incubated with 1:100 gold particles (10 nm, 5 nm, or 2 nm) goat anti-mouse for 1 hour. Finally, the grids were rinsed 4x with MilliQ and dried on filter paper. Silver enhancement of 2 nm gold particles was performed following Aurion R-Gent Silver Enhancement kit instructions.

Two different microscope systems were used. The TEM system, and a Supra 55 Scanning EM (Zeiss, Jena, Germany) with an X-max 150mm^2 silicon drift X-ray detector (Oxford Instruments, Abingdon, UK) which will hereafter be referred to as the SEM system. The imaging of 10 nm gold and 2 nm gold particles were performed with the TEM system and the 5 nm gold 2 nm gold plus silver imaging on the SEM system.

Metal-incorporation in diaminobenzidine reaction precipitates

The ER was genetically tagged with a FLIPPER comprised of GFP and horseradish peroxidase via PEI-transfection in Hek 293T cells. Prior to the DAB reaction, fixed cells were incubated with 20% weight/volume concentrations of metal solutions for 5 min. Then 10 mg DAB in 10 ml PBS, filtered through Whatman 0.2 µm filter with an additional 6 µl of 30% H_2O_2 was added to the cells for 20 min. Cells were further processed for EM in Durcupan resin. EDX acquisition was on the TEM system at 32.2k magnification with 512 by 512 pixels, 10 µs dwell time, 200 keV acceleration voltage, 5.42 nA current, and 241 frames.

Stains to paint cellular features

A 100-nm section of rat pancreas embedded in Durcupan was contrasted with 5% uranyl acetate for 20 min and Reynold's lead citrate for 2 min. Imaging was performed on the SEM system 30k magnification, 15 keV acceleration voltage, 7.5 mm working distance, 1 frame of 1024 x 832 pixels, process time 5, 1 ms dwell time EDX, and a 25° tilt.

All stains were applied to post-fixed rat pancreas tissue at 1% concentration in deionized water, except for mercury chloride which was a prepared solution of 0.5% and lead which was 1:3 dilution of Reynold's lead citrate. Tissue was embedded in EPON and 100-nm sections were collected on Formvar-coated carbon single hole sample holders. Sections were analyzed for EDX with the SEM system. EDX imaging was acquired with 15 keV acceleration voltage, specimen at a 25° tilt toward the detector, working distance of 4.2-6.3 mm, 50 µs dwell time, frames of 1024 x 832 pixels, except EDX imaging of lanthanum-stained tissue, which was acquired at a lower spectral resolution. The numbers of frames acquired are listed in **Table 2**. These experiments were performed during an explorative optimization period and therefore reflect use of two different holders: STEM carrousel (**Figure 5A, F, H, I**) and homemade EDX holders (described in [5]) (**Figure 5B-E, G, J**).

Fluorescent Probes

The fluorescent molecular probes listed in **Table 2** were added to HeLa cells in culture at the noted concentrations. For light imaging, cells were cultured on glass bottom petri dishes, fixed, imaged according to the manufacturer's guidelines then embedded in EPON, except for the cells with MitoTracker and rat pancreas tissue labeled with ATTO 514 which were embedded in Durcupan. Cells treated with BODIPY Cholesterol were fixed in a 1:1 mixture of fixative:2% osmium tetroxide. Sections were 100-nm thick on 1 mm hole carbon grids on formvar support film.

EDX imaging was performed on the TEM system (**Figure 6 A, C, D**) 200 keV; 10 us dwell time; spot size 5 and 512 x 512 pixels with current and frames as follows: MitoTracker Green sample at 5.46 nA, 290 frames; ReZolve ER sample at 4.87 nA, 364 frames; and IraZolve Mitosample at 4.40 nA current, 214 frames.

Samples imaged on the SEM system were imaged at 15 keV acceleration voltage, 5.6 nA current, process time 5, 5.4-5.6 mm working distance, 25° tilt toward X-ray detector, 50 µs dwell time, 22-30 frames of 1024 x 832 pixels. Frames of the BODIPY Cholesterol sample were 512 x 416 pixels.

Acknowledgements

Most of the work has been carried out at the UMC Groningen Microscopy & Imaging Center (UMIC), which is sponsored by The Netherlands organization for scientific research (ZonMW 91111.006; STW Microscopy Valley 12718; NWO 175-010-2009-023; *Netherlands Electron Microscopy Infrastructure* (*NEMI; NWO 184.034.014*). We would like to acknowledge the ThermoFisher Eindhoven NanoPort where all TEM data were acquired.

REFERENCES

1. Pirozzi NM, Hoogenboom JP, Giepmans BNG. ColorEM: Analytical electron microscopy for element-guided identification and imaging of the building blocks of life. *Histochem Cell Biol*. 2018.
2. Scotuzzi M, Kuipers J, Wensveen DI, et al. Multi-color electron microscopy by element-guided identification of cells, organelles and molecules. *Sci Rep*. 2017;7:45970.
3. Dasari S, Tchounwou PB. Cisplatin in cancer therapy: Molecular mechanisms of action. *Eur J Pharmacol*. 2014;740:364-378.
4. Wang D, Lippard SJ. Cellular processing of platinum anticancer drugs. *Nature Reviews Drug Discovery*. 2005;4(4):307-320.
5. Pirozzi NM, Kuipers J, Giepmans BNG. Chapter 5 - sample preparation for energy dispersive X-ray imaging of biological tissues. *Methods Cell Biol*. 2021;162:89-114. doi: https://doi-org.proxy-ub.rug.nl/10.1016/bs.mcb.2020.10.023.
6. Petrovic BV, Djuran MI, Bugarcic ZD. Binding of platinum(II) to some biologicaly important thiols. *Met Based Drugs*. 1999;6(6):355-360.
7. Svatoš A. Mass spectrometric imaging of small molecules. *Trends in Biotechnology*. 2010;28(8):425-434. doi: https://doi.org/10.1016/j.tibtech.2010.05.005.
8. Lee RFS, Riedel T, Escrig S, et al. Differences in cisplatin distribution in sensitive and resistant ovarian cancer cells: A TEM/NanoSIMS study. *Metallomics*. 2017(10):1413.
9. Lin Y, Wu K, Jia F, et al. Single cell imaging reveals cisplatin regulating interactions between transcription (co)factors and DNA. *Chem Sci*. 2021;12(15):5419-5429.
10. Rodilla V, Pertusa J, Pellicer JA. Ultrastructural localization of cisplatin in ehrlich ascites tumor cells. *Cancer Lett*. 1988;39(2):179-183. doi: https://doi.org/10.1016/0304-3835(88)90102-4.
11. Demir V, Bucher J, Kropf C, Arenz M, Segner H. Comparative study of cytotoxicity by platinum nanoparticles and ions in vitro systems based on fish cell lines. *Toxicology in Vitro*. 2020;66:104859. doi: https://doi.org/10.1016/j.tiv.2020.104859.
12. Jung M, Kim TK, Pack C, Mun JY. Immuno-gold techniques in biomedical sciences. In: Kim JK, Kim JK, Pack C, eds. *Advanced imaging and bio techniques for convergence science*. Singapore: Springer Singapore; 2021:133-152. https://doi.org/10.1007/978-981-33-6064-8_7. 10.1007/978-981-33-6064-8_7.
13. Deerinck TJ, Giepmans BN, Ellisman MH. Quantum dots as cellular probes for light and electron microscopy. *Microscopy and Microanalysis*. 2005;11 (S02):914-915.
14. Kuipers J, de Boer P, Giepmans BN. Scanning EM of non-heavy metal stained biosamples: Large-field of view, high contrast and highly efficient immunolabeling. *Exp Cell Res*. 2015;337(2):202-207.
15. Sjollema KA, Giepmans BNG. Automated annotating label in nanotomy - using ImageJ to quantify nanoparticles in large EM datasets. *Imaging and microscopy*. 2016;4(Nov):45-46.
16. Oliver C. Use of immunogold with silver enhancement. *Methods Mol Biol*. 2010;588:311-316.
17. Connolly CN, Futter CE, Gibson A, Hopkins CR, Cutler DF. Transport into and out of the golgi complex studied by transfecting cells with cDNAs encoding horseradish peroxidase. *J Cell Biol*. 1994;127(3):641-652.
18. Kuipers J, van Ham TJ, Kalicharan RD, et al. FLIPPER, a combinatorial probe for correlated live imaging and electron microscopy, allows identification and quantitative analysis of various cells and organelles. *Cell Tissue Res*. 2015;360(1):61-70.
19. Ramachandra R, Mackey MR, Hu J, et al. Elemental mapping of labelled biological specimens at intermediate energy loss in an energy-filtered TEM acquired using a direct detection device. *Journal of Microscopy*. 2021;n/a.

20. Adams JC. Heavy metal intensification of DAB-based HRP reaction product. *J Histochem Cytochem*. 1981;29(6):775.

21. Adams SR, Mackey MR, Ramachandra R, et al. Multicolor electron microscopy for simultaneous visualization of multiple molecular species. *Cell Chem Biol*. 2016;23(11):1417-1427.

22. Török I, Seprényi G, Pór E, Borbély E, Szögi T, Dobó E. Post-diaminobenzidine treatments for double stainings: Extension of sulfide-silver-gold intensification for light and fluorescent microscopy. *J Histochem Cytochem*. 2020;68(8):571-582.

23. Kuipers J, Giepmans BNG. Neodymium as an alternative contrast for uranium in electron microscopy. Histochem Cell Biol. 2020;153(4):271-277.

24. Novikov I, Subbot A, Turenok A, Mayanskiy N, Chebotar I. A rapid method of whole cell sample preparation for scanning electron microscopy using neodymium chloride. *Micron*. 2019;124:102687. doi: https://doi-org.proxy-ub.rug.nl/10.1016/j.micron.2019.102687.

25. Barnakov AN. Sequential treatment by phosphotungstic acid and uranyl acetate enhances the adherence of lipid membranes and membrane proteins to hydrophobic EM grids. *J Microsc*. 1994;175(Pt 2):171-174.

26. Ikeda K, Inoue K, Kanematsu S, Horiuchi Y, Park P. Enhanced effects of nonisotopic hafnium chloride in methanol as a substitute for uranyl acetate in TEM contrast of ultrastructure of fungal and plant cells. *Microsc Res Tech*. 2011;74(9):825-830.

27. Leitão RG, Silva MP, Diniz MS, Guerra M. Mapping the distribution of mercury (II) chloride in zebrafish organs by benchtop micro-energy dispersive X-ray fluorescence: A proof of concept. *Journal of Trace Elements in Medicine and Biology*. 2022;69:126874. doi: https://doi-org.proxy-ub.rug.nl/10.1016/j.jtemb.2021.126874.

28. Gillam TA, Sweetman MJ, Bader CA, et al. Bright lights down under: Metal ion complexes turning the spotlight on metabolic processes at the cellular level. *Coord Chem Rev*. 2018;375:234-255.

29. Bader CA, Sorvina A, Simpson PV, et al. Imaging nuclear, endoplasmic reticulum and plasma membrane events in real time. *FEBS Lett*. 2016;590(18):3051-3060.

30. Sorvina A, Bader CA, Darby JRT, et al. Mitochondrial imaging in live or fixed tissues using a luminescent iridium complex. *Sci Rep*. 2018;8(1):8191-018-24672-w.

31. Schanne G, Henry L, Ong HC, et al. Rhenium carbonyl complexes conjugated with methylated triphenylphosphonium cations as sensitive mitochondria trackers for X-ray fluorescence imaging. . 2021.

32. Lange F, Agüi-Gonzalez P, Riedel D, Phan NTN, Jakobs S, Rizzoli SO. Correlative fluorescence microscopy, transmission electron microscopy and secondary ion mass spectrometry (CLEM-SIMS) for cellular imaging. *PLOS ONE*. 2021;16(5):e0240768.